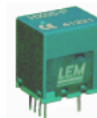


# LAMPIRAN



## Current Transducer HX 03 .. 50-P/SP2 $I_{PN} = 3 .. 50 A$

For the electronic measurement of currents: DC, AC, pulsed, mixed, with a galvanic isolation between the primary circuit (high power) and the secondary circuit (electronic circuit).



### Electrical data

Primary nominal r.m.s. current $I_{PN}$ (A)	Primary current measuring range $I_p$ (A) <sup>1)</sup>	Primary Conductor Diameter x Turns (mm)	Type
3	± 9	0.6d x 20T	HX 03-P/SP2
5	± 15	0.8d x 12T	HX 05-P/SP2
10	± 30	1.1d x 6T	HX 10-P/SP2
15	± 45	1.4d x 4T	HX 15-P/SP2
20	± 60	1.6d x 3T	HX 20-P/SP2
25	± 75	1.6d x 2T	HX 25-P/SP2
50	± 150	1.2 x 6.3 x 1T	HX 50-P/SP2

### Features

- Galvanic isolation between primary and secondary circuit
- Half effect measuring principle
- Isolation voltage 3000V
- Low power consumption
- Extended measuring range ( $3 \times I_{PN}$ )
- Single supply from +12V to +15V
- Material according to UL94-V0

$V_{OUT}$	Output voltage @ $\pm I_{PN}$ , $R_L = 2 k\Omega$ , $T_A = 25^\circ C$	$V_{OE} \pm 0.625$ V
$R_{OUT}$	Output impedance	< 50 $\Omega$
$R_L$	Load resistance	$\geq 2$ k $\Omega$
$V_C$	Supply voltage ( $\pm 5\%$ )	+12 .. +15 V
$I_C$	Current consumption	< 15 mA
$V_C$	R.m.s. voltage for AC isolation test, 50/60Hz, 1 mn > 3	> 3 kV
$V_e$	R.m.s. voltage for partial discharge extinction at 10pC	$\geq 1$ kV
	Impulse withstand voltage, 1.2/50 $\mu$ s	$\geq 6$ kV

### Advantages

- Low insertion losses
- Easy to mount with automatic handling system
- Small size and space saving
- Only one design for wide current ratings range
- High immunity to external interference.

### Accuracy-Dynamic performance data

$X$	Accuracy @ $I_{PN}$ , $T_A = 25^\circ C$ (without offset)	$\leq \pm 1$ % of $I_{PN}$
$\epsilon_L$	Linearity ( $0 .. \pm I_{PN}$ )	$< \pm 1$ % of $I_{PN}$
$V_{OE}$	Electrical offset voltage, $T_A = 25^\circ C$	$\pm 2.5V \pm 50$ mV
$V_{OH}$	Hysteresis offset voltage @ $I_p = 0$ ; after an excursion of $3 \times I_{PN}$	$< \pm 10$ mV
$V_{OT}$	Thermal drift of $V_{OE}$	max. $\pm 1.5$ mV/K
$TCE_g$	Thermal drift of the gain (% of reading)	$\pm 0.1$ %/K
$t_f$	Response time @ 90% of $I_p$	$\leq 3$ $\mu$ s
$f$	Frequency bandwidth (-3 dB) <sup>2)</sup>	50 kHz

### Applications

- Switched Mode Power Supplies (SMPS)
- AC variable speed drives
- Uninterruptible Power Supplies (UPS)
- Electrical appliances
- Battery supplied applications
- DC motor drives

### General data

$T_A$	Ambient operating temperature	- 25 .. + 85 $^\circ C$
$T_S$	Ambient storage temperature	- 25 .. + 85 $^\circ C$
$m$	Mass	8 g
	Min. internal creepage distance/clearance	$\geq 5.5$ mm
	Isolation material group	I
	Standards	EN50178

Notes : <sup>1)</sup> With  $R_L = 2k\Omega$

<sup>2)</sup> Small signal only to avoid excessive heating of the magnetic core

030806/3

LEM Components

www.lem.com

# TLP250

Transistor Inverter  
 Inverter For Air Conditioner  
 IGBT Gate Drive  
 Power MOS FET Gate Drive

The TOSHIBA TLP250 consists of a GaAlAs light emitting diode and a integrated photodetector.  
 This unit is 8-lead DIP package.  
 TLP250 is suitable for gate driving circuit of IGBT or power MOS FET.

- Input threshold current:  $I_F=5\text{mA}(\text{max.})$
- Supply current ( $I_{CC}$ ):  $11\text{mA}(\text{max.})$
- Supply voltage ( $V_{CC}$ ):  $10\text{--}35\text{V}$
- Output current ( $I_O$ ):  $\pm 1.5\text{A}(\text{max.})$
- Switching time ( $t_{pLH}/t_{pHL}$ ):  $0.5\mu\text{s}(\text{max.})$
- Isolation voltage:  $2500V_{\text{rms}}(\text{min.})$
- UL recognized: UL1577, file No.E67349
- Option(D4)

VDE Approved : DIN EN60747-5-2

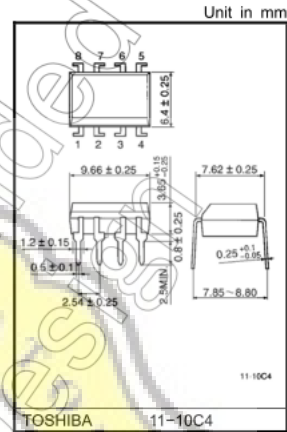
Maximum Operating Insulation Voltage :  $890V_{\text{PK}}$

Highest Permissible Over Voltage :  $4000V_{\text{PK}}$

(Note):When a EN60747-5-2 approved type is needed,  
 Please designate "Option(D4)"

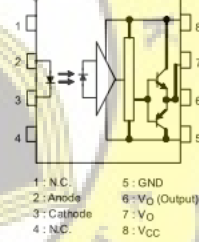
**Truth Table**

Input LED	$T_{r1}$		$T_{r2}$	
	On	On	Off	On
Off	Off	On	Off	On

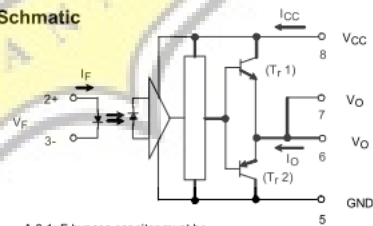


Weight: 0.54 g (typ.)

**Pin Configuration (top view)**



**Schematic**



A 0.1 $\mu\text{F}$  bypass capacitor must be connected between pin 8 and 5 (See Note 5).



# dsPIC30F4011/4012

## dsPIC30F4011/4012 Enhanced Flash 16-bit Digital Signal Controller

**Note:** This data sheet summarizes features of this group of dsPIC30F devices and is not intended to be a complete reference source. For more information on the CPU, peripherals, register descriptions and general device functionality, refer to the *dsPIC30F Family Reference Manual* (DS70046). For more information on the device instruction set and programming, refer to the *dsPIC30F Programmer's Reference Manual* (DS70030).

### High Performance Modified RISC CPU:

- Modified Harvard architecture
- C compiler optimized instruction set architecture with flexible addressing modes
- 84 base instructions
- 24-bit wide instructions, 16-bit wide data path
- 48 Kbytes on-chip Flash program space (16K instruction words)
- 2 Kbytes of on-chip data RAM
- 1 Kbytes of non-volatile data EEPROM
- Up to 30 MIPS operation:
  - DC to 40 MHz external clock input
  - 4 MHz-10 MHz oscillator input with PLL active (4x, 8x, 16x)
- 30 interrupt sources
  - 3 external interrupt sources
  - 8 user selectable priority levels for each interrupt source
  - 4 processor trap sources
- 16 x 16-bit working register array

### DSP Engine Features:

- Dual data fetch
- Accumulator write back for DSP operations
- Modulo and Bit-Reversed Addressing modes
- Two, 40-bit wide accumulators with optional saturation logic
- 17-bit x 17-bit single cycle hardware fractional/integer multiplier
- All DSP instructions single cycle
- $\pm$  16-bit single cycle shift

### Peripheral Features:

- High current sink/source I/O pins: 25 mA/25 mA
- Timer module with programmable prescaler:
  - Five 16-bit timers/counters; optionally pair 16-bit timers into 32-bit timer modules
- 16-bit Capture input functions
- 16-bit Compare/PWM output functions
- 3-wire SPI™ modules (supports 4 Frame modes)
- I<sup>2</sup>C™ module supports Multi-Master/Slave mode and 7-bit/10-bit addressing
- 2 UART modules with FIFO Buffers
- 1 CAN modules, 2.0B compliant

### Motor Control PWM Module Features:

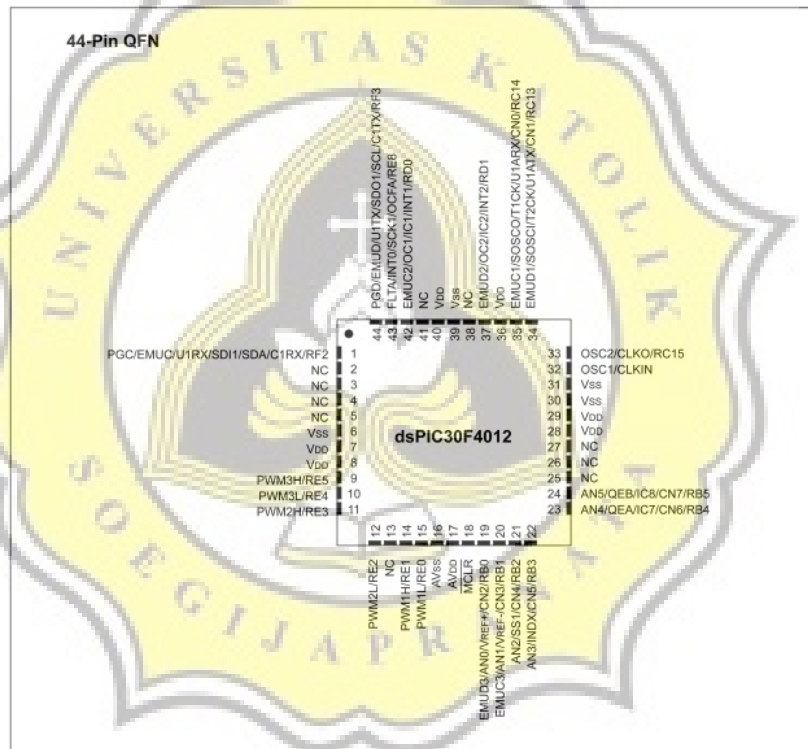
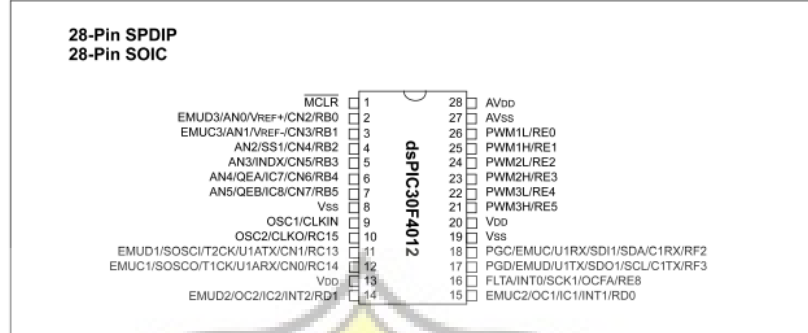
- 6 PWM output channels
  - Complementary or Independent Output modes
  - Edge and Center Aligned modes
- 3 duty cycle generators
- Dedicated time base
- Programmable output polarity
- Dead-time control for Complementary mode
- Manual output control
- Trigger for A/D conversions

### Quadrature Encoder Interface Module Features:

- Phase A, Phase B and Index Pulse input
- 16-bit up/down position counter
- Count direction status
- Position Measurement (x2 and x4) mode
- Programmable digital noise filters on inputs
- Alternate 16-bit Timer/Counter mode
- Interrupt on position counter rollover/underflow

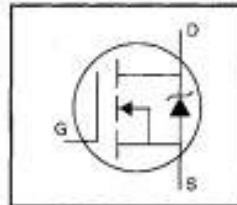
# dsPIC30F4011/4012

## Pin Diagrams (Continued)



HEXFET® Power MOSFET

- Dynamic dv/dt Rating
- Repetitive Avalanche Rated
- Isolated Central Mounting Hole
- Fast Switching
- Ease of Paralleling
- Simple Drive Requirements



$$V_{DSS} = 500V$$

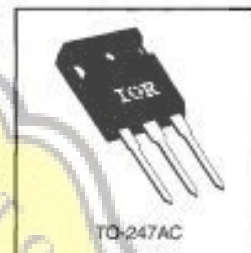
$$R_{DS(on)} = 0.27\Omega$$

$$I_D = 20A$$

**Description**

Third Generation HEXFETs from International Rectifier provide the designer with the best combination of fast switching, ruggedized device design, low on-resistance and cost-effectiveness.

The TO-247 package is preferred for commercial-industrial applications where higher power levels preclude the use of TO-220 devices. The TO-247 is similar but superior to the earlier TO-218 package because of its isolated mounting hole. It also provides greater creepage distance between pins to meet the requirements of most safety specifications.



DATA SHEETS

**Absolute Maximum Ratings**

Parameter	Max.	Units
$I_D @ T_C = 25^\circ C$ Continuous Drain Current, $V_{GS} @ 10V$	20	A
$I_D @ T_C = 100^\circ C$ Continuous Drain Current, $V_{GS} @ 10V$	13	A
$I_{DM}$ Pulsed Drain Current @	80	A
$P_D @ T_C = 25^\circ C$ Power Dissipation	280	W
Linear Derating Factor	2.2	W/°C
$V_{GS}$ Gate-to-Source Voltage	$\pm 20$	V
$E_{AS}$ Single Pulse Avalanche Energy @	960	mJ
$I_{AR}$ Avalanche Current @	20	A
$E_{AR}$ Repetitive Avalanche Energy @	28	mJ
dv/dt Peak Diode Recovery dv/dt @	3.5	V/ns
$T_J$ Operating Junction and Storage Temperature Range	-55 to +180	°C
Soldering Temperature, for 10 seconds	300 (1.8mm from case)	
Mounting Torque, 6-32 or M3 screw	10 lbf-in (1.1 N-m)	

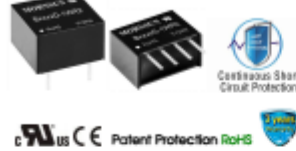
**Thermal Resistance**

Parameter	Min.	Typ.	Max.	Units
$R_{\theta JC}$ Junction-to-Case	—	—	0.45	°C/W
$R_{\theta CS}$ Case-to-Sink, Flat, Greased Surface	—	0.24	—	°C/W
$R_{\theta JA}$ Junction-to-Ambient	—	—	40	°C/W

DC/DC Converter  
B\_S-1WR2 & B\_D-1WR2 series



TW, Fixed input voltage, isolated & unregulated single output



FEATURES

- Continuous short-circuit protection
- Operating temperature range: -40°C to +105°C
- Conversion efficiency high up to 80%
- Miniature SP/DIP package, International standard pin-out
- Isolation voltage: 1.5K VDC
- EN60950, UL60950 Approval



B\_S-1WR2 & B\_D-1WR2 series are specially designed for applications where an isolated voltage is required in a distributed power supply system. They are suitable for:

1. Where the voltage of the input power supply is stable (voltage variation: ±10%V<sub>in</sub>)
2. Where isolation between input and output is necessary (isolation voltage: <1500VDC)
3. Where the output voltage regulation and the ripple & noise of the output voltage is not strictly required
4. Typical applications: digital circuit condition; normal low-frequency artificial circuit condition; relay drive circuit and data switching circuit condition, etc.

Certification	Part No.	Input Voltage (VDC)		Output		Efficiency (%) Min./Typ. @ Full Load	Max. Capacitive Load(μF)
		Nominal (Range)	Output Voltage (VDC)	Output Current (mA)(Max./Min.)			
UL/CE	B0005-1WR2	3.3 (2.7-3.3)	3.3	300/30	68/72	200	
	B0005-1WR2		5	200/20	72/75		
	B0125-1WR2		12	84/9	75/80		
	B0030-1WR2		3.3	300/30	68/72		
	B0030-1WR2		5	200/20	72/75		
	B0030-1WR2		3.3	300/30	68/72		
UL/CE	B0045-1WR2	5 (4.5-5.5)	5	200/20	72/75		
	B0045-1WR2		9	111/12	75/80		
	B0125-1WR2		12	84/9	75/80		
	B0185-1WR2		15	57/7	75/80		
	B0245-1WR2		24	42/4	75/80		
	B0030-1WR2		3.3	300/30	68/72		
UL/CE	B0030-1WR2	12 (10.8-13.2)	5	200/20	75/80		
	B0030-1WR2		9	111/12	75/80		
	B0120-1WR2		12	84/9	75/80		
	B0150-1WR2		15	57/7	75/80		
	B0240-1WR2		24	42/4	75/80		
	B0030-1WR2		3.3	300/30	68/72		
UL/CE	B1005-1WR2	5	5	200/20	75/80		
	B1005-1WR2		9	111/12	75/80		
	B1120-1WR2		12	84/9	75/80		
	B1150-1WR2		15	57/7	75/80		





SCORed 18




# CERTIFICATE OF PARTICIPATION

PRESENTED TO

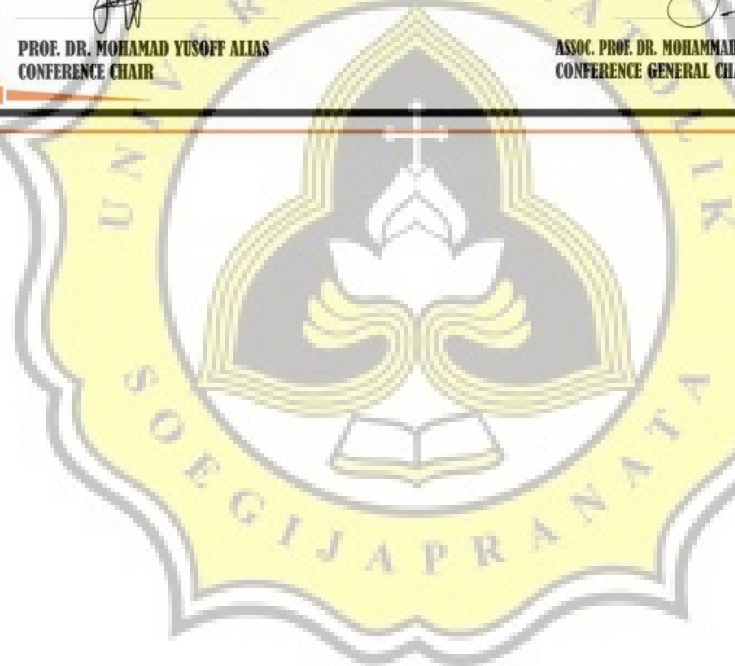
**ARDANTYA RAHARDIAN HARYAWAN**

FOR THE VALUABLE CONTRIBUTION AS  
**PRESENTER**

AT 2018 IEEE STUDENT CONFERENCE AND ON RESEARCH AND DEVELOPMENT (SCORED)  
AT BANGI GOLF RESORT, BANGI, MALAYSIA FROM THE 26TH TO THE 28TH OF NOVEMBER 2018

  
PROF. DR. MOHAMAD YUSOFF ALIAS  
CONFERENCE CHAIR

  
ASSOC. PROF. DR. MOHAMMAD FAIZAL AHMED FAUZI  
CONFERENCE GENERAL CHAIR



# Energy Efficient C-Dump Converter with Inductor for Switched Reluctance Motor

Ardantya Rahardian Haryawan, Slamet Riyadi  
Department of Electrical Engineering  
Soegijapranata Catholic University  
Semarang, Indonesia  
blogadiardan@gmail.com

**Abstract**— The electric motor is core in electric drives that is a very important element in electric vehicles. The switched reluctance motor offers some advantages in such applications, including simple construction and low cost. The converter is required to drive the switched reluctance motor because it needs sequential excitation on its phase windings. High torque is a requirement for electric motor needed in the electric vehicle. To minimize the negative torque, the phase current must be switched off fast after the negative slope of the phase inductance profile is started. It requires method to run through controlling the switching process and the exciting changes found in each winding phase. This topology has an inductor to limit the current during charging the capacitor to the DC voltage source. In this paper, will show about the commutation process and will explain the topology of energy efficient C-dump converter.

**Keywords**—electric motor drive; switched reluctance motor; C-dump converter; capacitor; energy efficeint; inductor

## I. INTRODUCTION

Nowadays, the use of fossil fuels in transportation is quite massive. Almost every vehicle currently uses fossil fuels. The negative impacts caused by the burning of these vehicles that is air pollution and the greenhouse effect which cause environmental damage [1]. In order to reduce the impact caused by these problems, the latest electric vehicle has been developed which uses a modern motor as its driving force.

Brushless DC motors (BLDC) are an example of today's modern drivers. Brushless DC motors have the advantage of being able to produce high torque. This motor also has several disadvantages such as complicated construction considering there are permanent magnets used in the rotor causes the motor has a larger size than other motor drives [2]. This motor is relatively more expensive, causing the lower interest of consumers. In order to overcome the disadvantages of brushless DC motor, switched reluctance motor (SRM) has been developed. This motor has advantages over Brushless DC motors. When viewed in terms of performance, switched reluctance motor can produce higher speeds and lower costs than brushless DC motor. Switched reluctance motor construction is simpler due to the absence of permanent magnets [3 - 4].

In order to control the switched reluctance motor requires a converter circuit. Currently, there are various types of converters. Each type of converter has its own characteristics,

especially C-dump converter. By using this converter, control technique will be easier and negative torque produced by the motor switched reluctance can be reduced. To reduce negative torque, converter will demagnetize the winding faster during the phase change process [5 - 6]. This paper presents Energy Efficient C-dump Converter topology.

## II. RESEARCH METHOD

Switched reluctance motor has the advantages found in the motor such as a simpler structure and low cost compared to Brushless DC because there are no permanent magnets embedded in the rotor. Switched reluctance motor is able to operate at variable temperatures.

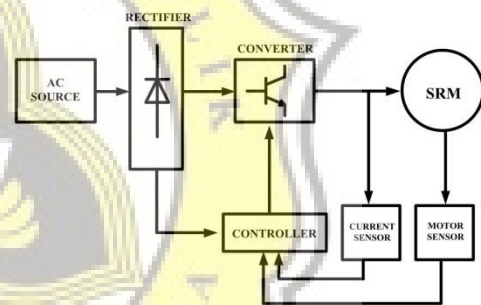


Fig. 1. Switched Reluctance Motor functional block diagram

The working principle of this motor is based on the difference of magnetic reluctance where the motor will receive a source voltage and producing a magnetic field in the stator winding and pulling the position of the nearest rotor and generating motor rotation. The number of rotor and stator in the motor is quite variant depending on the application. The number variants used on the side of the stators and rotors that have been made are 12/8. The number of stators and rotors will have an impact on the speed and torque. Switched reluctance motor drive has its own speed and torque characteristics compared to other types of drive motors [7]. The value of voltage and torque are presented in (1) and (2).



$$T(\phi, i) = \frac{1}{2} i^2 \frac{dL(\phi)}{d\phi} \quad (1)$$

$$V = i.R + \left( \frac{d\phi}{di} + \frac{di}{dt} \right) + \left( \frac{d\phi}{dt} + \frac{d\phi}{dt} \right) \quad (2)$$

Where  $i$  = The amount of current (Ampere)

The SRM torque equation is shown in Eq.(2). Decreased inductance in phase causes the torque is negative and increased inductance in phase causes the torque is positive. Based on this condition, if the phase inductance increased, the current will increase as much as possible. Therefore, phase change techniques are very required here. Adjusting the phase change can be done by controlling the switches [5 - 8].

Fig. 2, shows a circuit of energy efficient C-dump converters. The source voltage is separated from the demagnetization pathway. The converter will receive energy from the turns of each phase and flow directly into the capacitor. In this circuit, there is an inductor to limit the current during the use of the capacitor to the DC source voltage. The capacitor is used to store energy when the switch is turned off as prescribed [5 - 9].

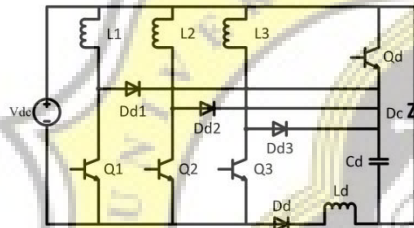


Fig. 2. Energy efficient C-dump converter circuit

When chopping mode, the converter will experience freewheeling mode past the switch  $Q_d$ . Switching  $Q_d$  will continue on if there is no specified command. When  $Q_d$  is OFF, the energy will flow to the capacitor until the voltage of the capacitor reaches the reference value then the  $Q_d$  is ON. In order to keep the current ripple not too high, the switching frequency must be increased. During the change in the voltage phase, the capacitor will continue to be maintained at the  $V_{DC}$  level. The change in voltage contained in the capacitor is inversely proportional to the value of the previous capacitor. The energy source from the per phase winding is fed to the capacitor dump before reaching an equal position. The voltage value of the capacitor dump is maintained twice the source voltage to produce a faster demagnetization process. The energy stored in the dump capacitor will be transferred to the source using the chopper operation as a buck converter. There are four switches that function as controls in several converter operating modes. The following are the four operating modes of this converter.

**A. Mode 1:  $Q_1$  and  $Q_d$  ON**

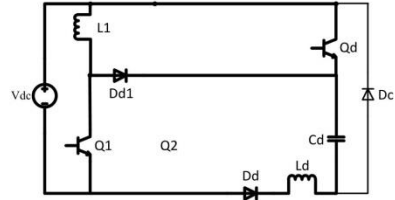


Fig. 3. Conduction mode of energy efficient C-dump converter

When conduction mode, phase current  $L_1$  will start to magnetize  $Q_1$  and  $Q_d$  ON then energy flows to the capacitor. Energy in the capacitor will flow to the source through the inductor  $L_d$ . The capacitor will supply voltage to the source, until the voltage on the capacitor drops. When the  $L_1$  phase has fulfilled by specified command, converter will run into chopping operation mode.

**B. Mode 2:  $Q_1$  OFF  $Q_d$  ON**

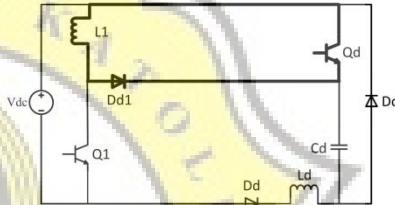


Fig. 4. Freewheeling mode of energy efficient C-dump Converter

After the conduction mode has reached the command value, then it will switch to freewheeling mode. The current of  $L_1$  flows into  $Q_d$  through diode  $D_{d1}$ . So the switch  $Q_d$  is temporarily turned on by waiting for the switching command. This mode will be maintained until the next mode turn to change, so current is maintained in predetermined conditions which are  $Q_d$  between on and off.

**C. Mode 3:  $Q_1$  and  $Q_d$  OFF (Commutation I)**

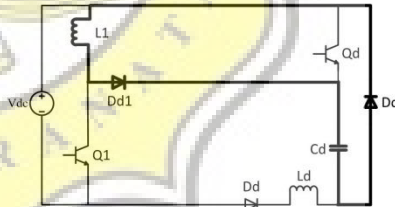


Fig. 5. Commutation mode I of energy efficient C-dump converter

When  $Q_1$  and  $Q_d$  OFF, the capacitor will receive and store energy through  $D_{d1}$ . The capacitor will continue to store and drain energy if the  $Q_d$  switch has not been turned on.

**D. Mode 4:  $Q_1$  OFF  $Q_2$  and  $Q_d$  ON (Commutation II)**

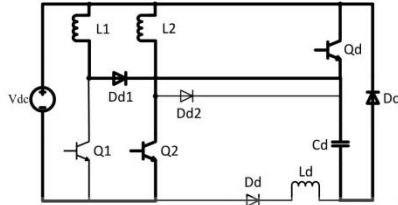


Fig. 6. Commutation mode II of energy efficient C-dump converter

Continue from commutation mode I,  $D_d$  diode will block the demagnetization current that flows through the DC source. When the  $L_1$  phase is demagnetizing, the  $L_2$  phase is magnetized by changing  $Q_2$  On. Freewheeling through the  $Q_d$  device does not start until the  $L_1$  phase fully demagnetized. During this period, the current through the  $L_2$  phase is maintained at the command value by removing extra energy into the capacitor. The results and analysis of C-dump converter data are presented in the following chapter III.

**III. RESULT AND DISCUSSION**

The C-dump converter has been simulated in PSIM software. The simulation has a prototype parameter of 100 volt on source voltage, capacitors is 5000uF, and 5mH for inductors. When it starts, the current and voltage will increase at the highest point where the capacitor reaches a voltage of 72 volts and resulting speed reached 830 rpm. After the converter experiences a commutation process, converter produces average peak results with a capacitor voltage of 252 volts and motor speed reaches around 2400 rpm. Can be seen in Fig. 9, which shows the voltage value of the capacitor. The switching process in the converter will affect the capacitor voltage. Capacitor shows fluctuating voltage due to the commutation process. From the simulation results that have been obtained, the higher the voltage value of the capacitor will have an impact on the result of motor speed. The results of the simulation output waveform are shown in the following figure.

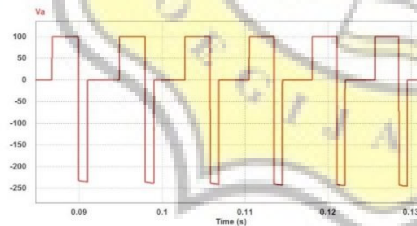


Fig. 7. Simulation result of phase A voltage ( $V_a$ )

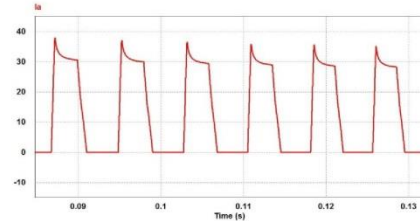


Fig. 8. Simulation result of phase A current ( $I_a$ )

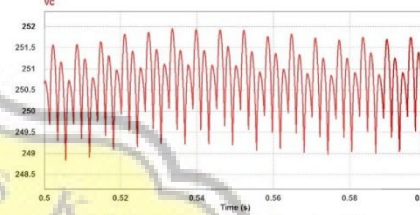


Fig. 9. Simulation result of capacitor voltage ( $V_c$ )

To minimize negative torque, the phase current must be switched off fast after the negative slope of the phase inductance profile is started as can be seen in Fig. 10, (black square).

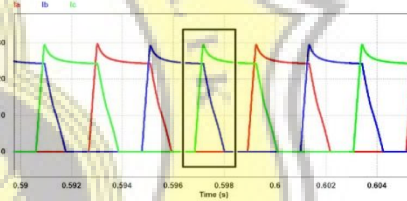


Fig. 10. Simulation result of three phases current

C-dump converters has been created and simulated in a laboratory where the parameters of the device have been set. Switched reluctance motor has 12/8 of the stator and rotor constructions. The source voltage of motor is supplied by 10V<sub>DC</sub> and the value of the capacitor is 470uF. The converter has four switching modes to control the converter. The switch on the C-dump converter uses MOSFET IRFP250 which capable of receiving voltages up to 250V<sub>DC</sub>. And for microprocessors using dsPIC30F4012. There are two reference values that have been determined as a comparison of the output. Both reference values are taken according to the ability of the device when it runs. With two comparisons the reference value produces its own output waveform. From this results, the lower of reference value will result a higher speed on switched reluctance motor and also increase its capacitor voltage.

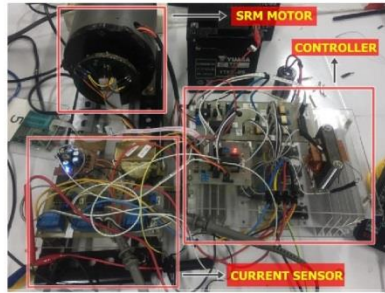


Fig. 11. Prototype hardware of C-dump converter for switched reluctance motor

The current of each phase is shown in Fig. 12. The voltage of each phase is shown in Fig. 13, and Fig. 14, shows the comparison between the source voltage and the capacitor voltage. The result of first reference value produces a capacitor voltage reaching 13 volts in excess of the source voltage of 10volt. At the first reference, the motor can produce a speed of 1300rpm.

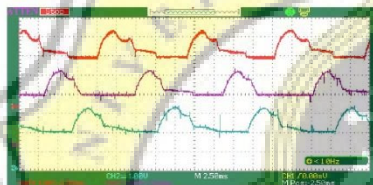


Fig. 12. Current each phase of experimental results

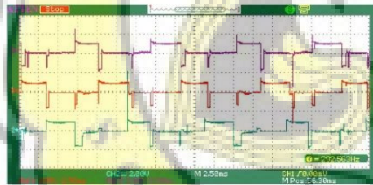


Fig. 13. Voltage each phase of experimental results (voltage scale 10x)

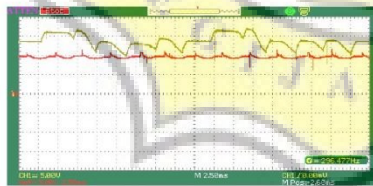


Fig. 14. Source voltage and capacitor voltage of experimental results

After getting the results from the first reference value, the second reference value will be used for comparison results.

The current of each phase is shown in Fig. 15, and the voltage of each phase is shown in Fig. 16. The source voltage and capacitor voltage are shown in Fig. 17. Second reference value shows the capacitor voltage is higher than the first reference value. The capacitor voltage reached 21 volts and the motor speed reached 2066 rpm.

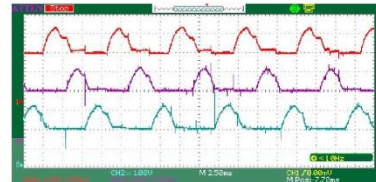


Fig. 15. Current each phase of experimental results

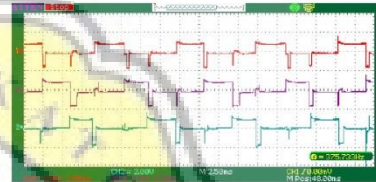


Fig. 16. Voltage each phase of experimental results (voltage scale 10x)

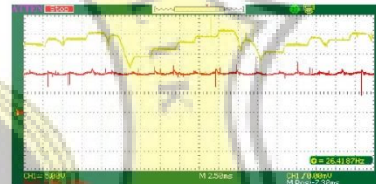


Fig. 17. Source voltage and capacitor voltage of experimental results

There are two operating modes of  $Q_d$  switch ON and OFF. When  $Q_d$  OFF, the energy is unable to flow in the  $Q_d$  switch and the capacitor will continue to receive energy from the source. This condition causes the capacitor to continue charging before  $Q_d$  is turned on as can be seen in the current of each phase, the intersection of the current can be turned off faster.

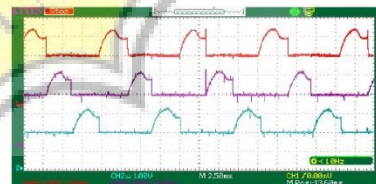


Fig. 18. Current each phase of experimental results  $Q_d$  OFF



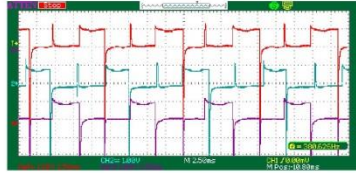


Fig. 19. Voltage each phase of experimental results  $Q_d$  OFF (voltage scale 10x)

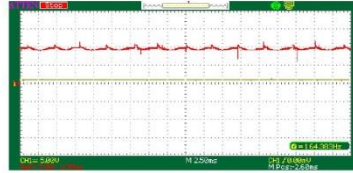


Fig. 23. Source voltage and voltage capacitor of experimental results  $Q_d$  ON

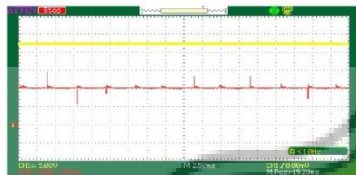


Fig. 20. Source voltage and capacitor voltage of experimental results  $Q_d$  OFF (voltage scale of capacitor 10x)

When  $Q_d$  ON, the current that has flowed past the capacitor will flow to the  $Q_d$  switch. It can be seen in Fig. 23, that the capacitor did not receive the voltage from the source. For the current wave of each phase in Fig. 21, is different from the condition when  $Q_d$  OFF, intersection of current when  $Q_d$  is slower is turned off than when  $Q_d$  is off.

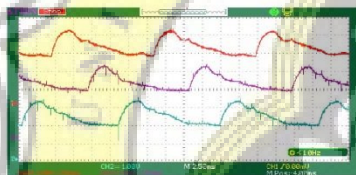


Fig. 21. Current each phase of experimental results  $Q_d$  ON

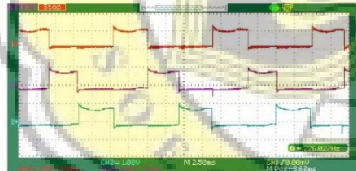


Fig. 22. Voltage each phase of experimental results  $Q_d$  ON (voltage scale 10x)

#### IV. CONCLUSIONS

The energy efficient of C-dump converter with inductors make one of the converters used to drive Switched Reluctance Motor. With control techniques using several predetermined reference values, there are two reference values as a comparison. The higher the voltage values on the capacitor, the higher the speed produced by switched reluctance motor. This converter can reduce the negative torque by accelerating the changing process of switching each phase.

#### REFERENCES

- [1] A.H.M Sadrul Ula, "Global Warming And Electric Power Generation: What Is The Connection?", IEEE Transactions On Energy Conversion, Vol. 6, No. 4, December 1991.
- [2] Md. Rifat Hazari, Effat Jahan, Md. Ebtaker Siraj, Md. Tauhedull Islam Khan and Ahmed Moruza Saleque, "Design of a Brushless DC (BLDC) Motor controller", International Conference on Electrical Engineering and Information & Communication Technology (ICEEICT), April 2014.
- [3] Jung-Moo Seo, Joo-Han Kim, and In-Soung Jung, "Design and Analysis of Slotless Brushless DC Motor", IEEE Transactions on Industry Applications, Vol. 47, No. 2, March/April 2011.
- [4] Ibrahim Sengor, Abdullah Polat, and Lale T. Ergene, "Design and analysis of switched reluctance motors", International Conference on Electrical and Electronics Engineering, November 2013.
- [5] Sayeed Mir, Iqbal Husain, and Malik E. Elbuluk, "Energy Efficient C-Dump Converter For Switched Reluctance Motor", IEEE Transactions On Industrial Electronics, Vol. 12, September 1997, pp. 912-921.
- [6] H. Bagherian, M. Asgar, and E. Afjei, "A New C-Dump Converter For Bifilar Winding Switched Reluctance Motor", IEEE Conference, Drive System and Technologies, February 2011.
- [7] K. Vijayakumar, R. Karthikeyan, S. Paramasivam, R. Arumugam, and K.N. Srinivas, "Switched Reluctance Motor Modeling, Design, Simulation, and Analysis: A Comprehensive Review", IEEE Transactions On Magnetics, Vol. 44, No. 12, December 2008.
- [8] F. Faradjizadeh, M. R. Tavakoli, M. Salehnia, and E. Afjei, "C-Dump Converter for Switched Reluctance Generator" IEEE Conference, Drive System and Technology, February 2014.
- [9] Prebin Babu B and Jayan M.V, "A High Efficiency Novel C-Dump Topology base Converter for SRM", IEEE International Conference on Power, Control, Signals and Instrumentation Engineering (ICPCSI), September 2017.

7.89<sup>6</sup>/<sub>2</sub> 6

### FORMULIR SCAN ANTI PLAGIARISME

Nama : Ardantya Raherdian Haryawen

Alamat email : blogadiardan@gmail.com

Fak. / Prodi : Teknik Elektro NIM: 14.F1.2015

berupa ( TESIS, TUGAS AKHIR, SKRIPSI, SUMMARY, LAPORAN KERJA PRAKTEK )

dengan judul : DESAIN KONVERTER L-DUMP TIPE

ENERGY EFFICIENT UNTUK MOTOR SWITCHED RELUCTANCE

.....

Semarang  
Petugas



Yang Menyerahkan,

Dosen Pembimbing,

NB. Laporan hasil scan terlampir

untuk Yang bersangkutan \*





## Doc vs Internet + Library

92.17% Originality	7.83% Similarity	30 Sources
--------------------	------------------	------------

### Web sources: 5 sources found

1. <a href="http://eprints.ums.ac.id/813/2/B200040071.pdf">http://eprints.ums.ac.id/813/2/B200040071.pdf</a>	0.15%
2. <a href="http://repository.uinjkt.ac.id/dspace/bitstream/128456789/30648/1/FARID%20FADZ%20-%20FSH...">http://repository.uinjkt.ac.id/dspace/bitstream/128456789/30648/1/FARID%20FADZ%20-%20FSH...</a>	0.15%
3. <a href="https://www.slideshare.net/ridwanpasmadavikerschikazekageva/bab-12-32489834">https://www.slideshare.net/ridwanpasmadavikerschikazekageva/bab-12-32489834</a>	0.14%
4. <a href="https://id.scribd.com/doc/21512730/Avr-Untuk-Generator-Sinkron-3-Fasa">https://id.scribd.com/doc/21512730/Avr-Untuk-Generator-Sinkron-3-Fasa</a>	0.14%
5. <a href="https://ml.scribd.com/doc/21512730/Avr-Untuk-Generator-Sinkron-3-Fasa">https://ml.scribd.com/doc/21512730/Avr-Untuk-Generator-Sinkron-3-Fasa</a>	0.14%

### Library sources: 25 sources found

13.50.0017 Sabar Santoso.docx	3.76%
Denis Adi Surya Tj 13.50.0006.doc	3.59%
KONVERTER C-DUMP TANPA INDUKTOR UNTUK PENGGERAK MOTOR SWITCH.doc	2.65%
13.50.0009 Naomi Intan H.docx	2.43%
KHO LUKAS BUDI SETIAWAN ANALISA TEGANGAN KAPASITOR PADA KON.doc	2.12%
13.50.0013 Hendra Winarto.doc	2.1%
13.50.0023 Gregorius Ganang Setyo Utomo.doc	1.85%
13.50.0020 - Agustinus Dian Purnadi.doc	1.73%
13.50.0022 Mario Purwa Negara.doc	1.64%
13.50.0012 - Alvin Dharmawan Sugianto.doc	1.62%
13.50.0012 - Alvin Dharmawan Sugianto II.doc	1.62%
13.50.0002 - Indrian haryanto.doc	1.42%
13.50.0010 - YOSUA IVAN PURNAMA.docx	0.92%
13.50.0004 - ABRAM ALAM SUHARDI.docx	0.87%
13.50.0016 - STEFANUS KRISTIAN ANDREANTO.docx	0.87%
14.F1.0026 Natanael Novialutli.docx	0.85%
14.F1.0010 Wira Adhitama.docx	0.68%
10.50.0020 Putera Adityas.docx	0.6%
14.F1.0026 Natanael (revisi).docx	0.39%
16.H1.0043 AHMADI YOGI PRATAMA.docx.docx	0.15%
16.H1.0043 AHMADI YOGI PRATAMA.docx	0.15%
Sigma Prabandaru 13.12.0073.docx	0.14%
MAHARANI LINTANG SIWI 27 Maret.docx	0.14%
TEGAR STARRYSTIA 27 Maret.docx	0.14%
16.H1.0018_Maria Sri.docx.docx	0.14%

 Similarity	 Citation
 Similarity from a chosen source	 References
 Possible character replacement	